Rapid reformatting of the cortical code during active tactile discrimination

Evan R. Harrell[1,2,*], Anthony Renard[1,2], and Brice Bathellier[1,2*]

[1] Department for Integrative and Computational Neuroscience (ICN)
Paris-Saclay Institute of Neuroscience (NeuroPSI)
UMR9197 CNRS/University Paris Sud
CNRS, Building 32/33, 1 avenue de la Terrasse, 91190 Gif-sur-Yvette, France

[2] Institut Pasteur, INSERM, Institut de l'Audition, 63 rue de Charenton, F-75012 Paris, France.

* Corresponding authors: evan.harrell@unic.cnrs-gif.fr, brice.bathellier@cnrs.fr

Abstract

Touch-based object recognition relies on perception of compositional tactile features like roughness, shape, and orientation. However, it remains unclear how the underlying spatio-temporal information from tactile sensors is integrated to form such percepts. Here, we establish a barrel cortex-dependent perceptual task in which mice use their whiskers to discriminate tactile gratings based on orientation. Multi-electrode recordings in barrel cortex during task performance reveal weak orientation tuning in the firing rate of single neurons during grating exploration despite high cortical firing rates. However, population-based classifiers decode grating orientation in line with concurrent psychophysical measurements and correlate with decisions on a trial-by-trial basis. For better decoding performance, the precise temporal sequence of population activity is necessary during grating exploration but becomes dispensable after decision. Our results suggest that temporal sequences of activity in barrel cortex carry orientation information during exploration. This code is reformatted around decision time to make firing rates more informative.

Introduction

Touch-based object recognition is essential for guiding behavior in a wide variety of environmental conditions. Reliable recognition generally depends on tactile search behavior executed with appendages like fingers for humans or the mystacial vibrissae for rodents[1]. The vibrissae, or whiskers, are rooted on the rodent snout in densely innervated follicles, where mechano-sensitive cells transduce whisker bending and contact forces into electrical signals[2]. The resulting sensory information has spatial (across whiskers) and temporal aspects that are integrated as it passes through several distinct somatosensory pathways before reaching barrel cortex and other areas[3]. As the foremost recipient of primary somatosensory thalamic afferents[4], barrel cortex is seen as the major cortical hub for the processing of whisker-based tactile information[5]. However, its precise functional roles remain poorly understood, as it has been difficult to disentangle the multiplexed encoding of whisker touches and self-generated movement[6].

Extensive studies on how barrel cortex neurons respond to simple, reliably targeted whisker stimuli have revealed a somato-topographical code based on high velocity deflections of one or several whiskers[7]. However, behavioral studies suggest this simple coding framework is not sufficient to support some of the perceptual functions of barrel cortex. In head-fixed mice, barrel cortex indispensably encodes the precise location of an object in a task requiring whisker search behavior[8,9]. This simple feature, location, is already beyond what a code based purely on velocity can represent for a single whisker. Although barrel cortex is essential to precisely localize objects, it is not required to actively detect the presence or absence of objects in the proximal surroundings[10,11]. This simpler detection process can likely be supported by other brain areas. In more demanding task conditions like the discrimination of

sandpapers[12–15] or in situations that require cognitive planning like whisker-mediated gap crossing[10], barrel cortex is once again essential. Taken together, perceptual studies suggest that barrel cortex is critical for precisely placing and recognizing tactile objects, especially in conditions that demand spatial and temporal integration of tactile inputs. The simple coding schemes generated from reliably targeted whisker stimuli do not shed light on how barrel cortex serves these perceptual processes.

To better understand the neural underpinnings of tactile object recognition, it is thus crucial to study how barrel cortex integrates tactile information across space (whiskers) and time to encode segregating tactile features. In this pursuit, many studies have focused on how the coarseness of anisotropic surface textures (sandpapers) is encoded during exploration with one or a few whiskers[12–16]. These studies have suggested that object coarseness is encoded by temporal integration of whisker slip events, with higher rates of slip events causing higher firing rates in barrel cortex[15–18]. While these studies have given important insights, coarseness is just one feature that can differ between objects. Along with variations in coarseness, natural objects also exhibit unique combinations of large-scale isotropic features, which means they can be decomposed into an arrangement of oriented surfaces. While it is documented that rats can discriminate oriented tactile gratings with their whiskers[19], it is not known if and how information about grating orientation is encoded in barrel cortex during active sensation. To study this, we developed a barrel cortex-dependent Go/NoGo task in which head-fixed mice discriminate tactile gratings based on orientation with their whiskers. Multi-electrode recordings during task performance revealed that during peak cortical firing rates in the early phase of grating exploration, few single neurons showed any orientation selectivity. However, support vector machine (SVM) classifiers based on the time course of population

activity in this period decoded the orientation category in line with concurrent psychophysical measurements. Examination of hit, false alarm, and correct rejection trials indicated that when the mice correctly classified the grating, decoders based on the barrel cortex activity also performed best at discriminating the gratings, and this could not be explained only by differences in licking behavior that are inherent in the Go/NoGo paradigm. As decisive licking ensued, single neuron firing rates became more informative. These results suggest that orientation information is first encoded by a temporal sequence of population activity in barrel cortex, which reflects the gathering of information associated with active object search. Then, as decision nears, higher level processing makes single neuron firing rates more informative.

Results

Mice categorize texture gratings based on orientation

It has recently been shown that freely moving rats can discriminate the orientation of tactile gratings with their whiskers[19]. To investigate if mice are also able to perform this discrimination, we trained head-fixed, water-deprived mice (**Fig. 1a, Supplementary Fig. 1**) to report the perceived orientation of a tactile grating by licking a tube to receive a water reward. The oriented gratings were presented in full dark conditions using a linear stage, and on some days all whisker interactions with the gratings were filmed with a high-speed infrared video camera (see Methods). For each trial, after no licking was detected on the reward port for at least 3 seconds, a 2 kHz sound was played to signify trial onset and a grating was translated into reach of the right whisker field (**Fig. 1b**). After a 1 second period of interaction with the grating, mice reported the orientation of the grating by either licking to obtain a water reward (Go trial) or refraining from licking to avoid punishment (**Fig. 1b**). In these trial

conditions, mice were trained to perform a simple Go/NoGo discrimination between a vertically oriented grating (90°) and a horizontal grating (0°), with Go and NoGo stimulus types interchanged in different groups of animals (**Supplementary Fig. 1** and Methods for all training details). After performance of simple Go/NoGo discrimination stabilized above 70% correct across 2 days, intermediate orientation angles spaced by 9° were gradually introduced and reinforced (**Fig. 1b**, see Methods). In this psychometric version of the task, the boundary between rewarded and non-rewarded orientations was 45°, and the fully ambiguous orientation was never presented.

From the beginning of simple Go/NoGo (0° vs. 90°) training, mice quickly learned the appropriate time to lick and after 10-15 days (~2000 trials), they easily discriminated between orthogonal grating orientations as measured by their licking behavior (**Fig. 1c**). Improved performance across time was mostly attributable to refraining from licking for the NoGo stimuli (**Fig. 1c**). After progressing to the psychometric version of the task, the ongoing motivational state of the animal, driven by thirst, determined whether False Alarm or Miss errors were more common. In most animals, we observed a more gradual change in licking behavior across orientation steps for NoGo than for Go orientations **(Fig. 1d**, lick histograms). Along with this, mice tended to make more False Alarm errors than Miss errors (**Fig. 1d**) indicative of a strategy aiming to minimize reward loss. This strategy results in asymmetric psychometric functions (**Fig. 1d**). To balance these curves[20], we averaged across animals in which the Go and NoGo orientations had been interchanged, and this revealed that the discrimination performance controlled for motivation is almost perfectly symmetric (**Fig. 1d**). These results confirm that like

rats[19], mice can discriminate tactile gratings using only their whiskers, and they do so with high acuity.

Barrel cortex is essential for discriminating oriented gratings

After establishing that mice can discriminate oriented gratings with their whiskers, we asked if barrel cortex is essential to perform the simple Go/NoGo version of this task. Optogenetic manipulations can perturb performance even if a brain area is dispensable[11], so we opted for a barrel cortex lesioning strategy. Mice were trained in the simple Go/NoGo version of the task until they reached stable performance above 70% correct across 2 days, after which thermo-coagulation lesions[21] were applied over the entire contralateral postero-medial barrel field (**Fig. 2a**, **Supplementary Fig. 2**). As a control, another group of animals (sham group) underwent mock surgeries that involved the same duration of anesthesia, a large craniotomy over barrel cortex, and the same process to reseal the exposed brain but with no lesion. The day after surgery, both lesion and sham groups performed the simple Go/NoGo task at chance levels (**Fig. 2b**), indicating that the general aftereffects of surgery and craniotomy have an impact on performance. Over the ensuing days, the sham group steadily recovered performance, while the lesioned group continued to perform at chance levels (**Fig. 2b**). Lesions were examined post hoc in coronal sections to assure that all postero-medial barrels (straddlers, A1-E4) in the whisker region of the primary somatosensory cortex had been removed (**Supplementary Fig. 2**).

Barrel cortex lesions are known to affect whisker movement control[11,22]. Therefore, we examined high-speed videos of whisker movements executed by the animals during task performance in sham and lesion groups. To quantify global

whisker movements throughout a trial, we defined the whisking envelope as the rectified and smoothed centroid velocity of the binarized whisker image within a manually traced ROI around the whisker bases (**Fig. 2c**, See Methods). This envelope showed that whisking behavior is most pronounced between trial onset (trial start sound cue) and the time when the grating is fixed and within reach of the whiskers (**Fig. 2d**). Surgery affected the average whisking envelope in both sham and lesion groups of animals, as quantified by the total whisking at trial onset (**Fig. 2e**, area under the whisking envelope curve). By day 3 after surgery, the total whisking of both groups returned to pre-surgical levels, but the behavioral performance recovered only in the sham group. Therefore, the drop in task performance after lesion cannot be explained by deficiencies in global whisker control. Barrel cortex removal also did not impact performance by abolishing licking. On day 3 after surgery, hit rates and false alarm rates were equal in the lesioned animals (both at ~50%), indicating that mice randomly licked rather than never licking at all, which would both produce chance level performance (**Fig. 2f**). These results indicate that intact barrel cortex is required to discriminate grating orientations with the whiskers, and this cannot be explained by changes in global whisker search behavior or licking ability.

Discrimination performance correlates with exploratory whisking and increased barrel cortex spiking activity

To study the encoding of grating orientation in mouse barrel cortex during active discrimination, we made acute extracellular recordings (9 recordings, 74 single unit and 274 multi-units) during the psychometric Go/NoGo version of the task (**Fig. 3a**, **Supplementary Fig. 3**). Silicon probes with linearly spaced electrodes (spanning

775 µm) were lowered to 1 mm depth from the surface of the contralateral barrel cortex (targeted C2 whisker A/P: -1.5mm, M/L: 0/3.3mm). Electrode placement in the barrel cortex was histologically verified in tangential sections after the experiments (**Supplementary Fig. 3**), and most of the active cells that were recorded resided in deeper layers (**Supplementary Fig. 3**). All recorded mice showed stable task performance above 70% correct on the day before the recording, but only some of them went on to perform during the recording (n=5 discriminating mice), while others did not (n=4 non-discriminating mice). This is likely due to the anesthesia, durotomy, and electrode descent preceding behavioral measurements in these acutely recorded animals.

In an example hit trial from a discriminating animal (**Fig. 3b**), the mouse initiated whisking before the grating came into reach and spiking activity increased once the grating was close enough to touch the whiskers. After ~500 ms of exploration, the mouse decided to lick and received a water reward, which triggered prolonged licking. In an example correct rejection trial (**Fig. 3c**), the same mouse also whisked into the grating, which produced spiking activity in the last ~250 milliseconds before the grating stabilized at its fixed position in reach. Then, the mouse correctly withheld licking to avoid punishment. This same behavioral sequence was apparent when averaging across all trials in this animal (**Fig. 3d**) or across all discriminating animals (**Fig. 3e**). As the grating approached the mice, they executed whisker search behavior, which was followed by a burst of spiking activity in barrel cortex neurons that peaked just before the grating stopped near the snout. Licking was initiated after the grating stopped and became discriminative ~590 ms after the peak of population activity (**Fig. 3e**). After the decision to lick, low whisking levels were maintained and,

in some mice, a rebound of whisking and barrel cortex activity was observed when the texture moved out of reach (**Fig. 3e**).

These patterns of behavior were much less discernible in animals that did not discriminate the gratings during the recording (**Fig. 3f-g**). In these animals, licking was initiated earlier, even before the grating came to a halt, indicating that their choice behavior did not take the grating into account. Whisking levels and spiking activity were also reduced, especially during the early interactions with the grating. However, the population firing rates still peaked just before the grating arrived at its fixed position, suggesting that there could be orientation-related information present in the barrel cortex at that time point even if these animals did act on it. These data indicate that patterned behavior and spiking activity in barrel cortex are associated with task performance.

Temporal decoders reproduce psychophysical measurements and outperform rate decoders during object search

We next quantified the information about grating orientation that is present in sample populations of barrel cortex neurons during task performance. To do this, we trained support vector machine (SVM) classifiers using a leave-one-trial-out cross-validation procedure for each mouse based on the activity of simultaneously recorded single and multi-units (**Fig. 4a**). The classifiers were then applied to decode the orientation category of the left-out trial (>45° or <45°), and this procedure was repeated until every trial had been left-out. Because tactile inputs occur in a series of multi-whisker contacts that evoke dynamic cortical responses, we examined whether a temporal code was present by basing the classifiers on population vectors spanning 5 consecutive 100 ms time bins of spiking activity (**Fig. 4a)**. To assess the

contribution of spike timing, we also trained classifiers with a single 500 ms bin (**Fig. 4b**, average firing rate). At trial onset, there was no information about grating orientation in the barrel cortex spiking activity and both types of classifiers performed at chance levels (50%). As the texture moved into range of the whiskers, performance improved rapidly for the temporal decoders, and sluggishly for the average firing rate decoders (**Fig. 4a-b**). This improvement happened well before discriminative licking for the temporal decoders (**Fig. 4a-b**), and therefore cannot be related to lick-induced whisker movements against the gratings. The elevated early performance of temporal decoders was consistent across many bin sizes that could be chosen for the population vectors (**Supplementary Fig. S4**, 50 ms and 25 ms).

If the grating orientation information encoded in barrel cortex is relevant for orientation perception, the decoders should produce neurometric functions that resemble the psychophysics exhibited by the animals. To check this, we computed classifier neurometric functions by examining performance across grating orientation angles (**Fig. 4c)**. In the 500 ms period before discriminative licking (See Methods), which we defined as the early period (always portrayed in blue comprising the end of whisker search, which is shown in pale blue), the temporal decoders generated neurometric functions that were more similar to the psychometric behavior than the average firing rate decoders (**Fig. 4c left).** After feedback in the form of reward or punishment (late period), both types of decoders performed equally well in matching the psychometric behavior (**Fig. 4c right**). To confirm the temporal nature of the code while controlling for the number of dimensions in the classifiers, we shuffled the temporal order of the population vector bins for the tested trial and examined how that affected classifier performance. The correct bin order had a clear advantage during the early period, but during the late period temporal shuffling had no effect on

classifier performance (**Fig. 4d**). Shuffling the cell identities in the same fashion abolished almost all classifier performance at any time relative to trial onset, indicating that unit identity is also important for grating orientation encoding (**Fig. 4d**).

Another way to verify that spike timing is important during the early period is to vary the training and testing times of the classifiers and observe how the shifts degrade the classifier performance. We trained temporal decoders at one time point and tested them at all other time points. During the early period, small misalignments in time completely abolished the decoding power of the classifiers (**Fig. 4e, left**) indicative of a code in which latency and/or temporal sequences are paramount. During the late period, the classifier was much more robust to time shifts indicating a more stable code, consistent with the decreased role of temporal information in this period. Taken together, these analyses suggest that at the onset of object search, information about grating orientation is present in the temporal sequence of population activity, and with time this code stabilizes into a firing rate code. These relationships do not hold in animals that do not discriminate the gratings (**Fig. 4e**). Along with highlighting the increased performance of temporal decoders during search behavior, these results affirm that the activity in barrel cortex encodes information about grating orientation.

Orientation tuning is weak at the onset of barrel cortex spiking responses but increases as licking sets in

While population-based classifiers can quantify the grating orientation information present across sample populations of barrel cortex neurons, they do not shed light on if and how single cells or small groups of cells encode grating orientation. Looking at some single unit activity, some discharged many spikes at the

onset of whisker interactions with the grating, and their firing rates then adapted when the grating reached its fixed position (**Fig. 5a**, **Supplementary Fig. 3**, Single Unit 1). Other neurons had less pronounced onset responses, but still had elevated firing rates while the grating was within reach (**Fig. 5a**, **Supplementary Fig. 3**, Single Unit 2). To quantify these responses, we constructed orientation tuning curves in 500 ms windows at different latencies with respect to trial onset (**Fig. 5b, Supplementary Fig. 5**, blue-magenta gradient). Tuning curves were computed for single units and multi-units by summing the spikes within a 500 ms window of interest for each trial of a given orientation, then dividing the total number of spikes for each trial by the size of the window (500 ms) (**Fig. 5b, Supplementary Fig. 5**, 6 examples**)**. The mean and standard deviation of these firing rates across trials for Single Unit 1 (same unit as **Fig. 5a** top) showed little selectivity for grating orientation during the peak firing of the early response (**Fig. 5b** top left, blue) or the late period after discriminative choice (**Fig. 5b** top left, magenta). To assess turning significance, we expressed the tuning curves in polar form and compared the magnitude of the vector sum to the vector sums obtained from shuffling the trial labels 200 times (**Fig. 5b** bottom left). If the actual tuning vector was further away from the mean of the shuffles than 95% of the shuffles, it was considered significant (False positive rates 5%). For Single Unit 2 (same unit as **Fig. 5a** bottom), orientation tuning was significant according to our shuffling procedure (**Fig. 5b** right). This unit had delayed responses compared to the peak of population activity that occurred just before the grating halted within range of the whiskers. The orientation tuning originated in the second 500 ms time bin after the start of the search period, and it persisted through discriminative choice and feedback. Examining the orientation tuning across time for all single and multi-units, we found that tuning was not above chance levels during the peak of firing that

occurs just before grating halt, and started to appear in the short period between grating halt and discriminative licking (**Fig. 5c**). Temporal decoders already have performance above chance and average firing rate decoders perform poorly during this period (**Fig. 4b-c**). These analyses suggest that during object search, information about grating orientation is not well-encoded by the firing rate of single neurons. Rather, it begins in a dynamic temporal sequence of population activity in barrel cortex associated with peak cortical firing rates, after which orientation tuning builds up as discriminative licking sets in. In non-discriminating animals, there are fewer responsive cells in barrel cortex and also much fewer tuned cells in all periods (**Fig. 5c** bottom right). Taken together, these results suggest that early responses represent information about orientation at the population level and depend on the timing of spikes. Later, orientation tuning increases and single neuron firing rates become more informative, and this transformation likely requires downstream temporal integration.

Barrel cortex activity encodes trial outcome for correct decisions on a trial-by-trial basis controlling for licking

An important final step in establishing a link between barrel cortex activity and orientation perception is to show that the barrel cortex encoding varies along with the animal's choices on a trial-by-trial basis. This can be done by examining the barrel cortex encoding across different trial outcomes, which in our case were Hits, Misses, False Alarms and Correct Rejections (**Fig. 6a**, example animal). Because most animals performed very few Misses, we concentrated on Hit, False Alarm, and Correct Rejections for this analysis (**Fig. 6b**, example animal). Looking at a single discriminating mouse, the trial-averaged whisking envelopes and population firing

rates differed across time for different trial outcomes (**Fig. 6a-b**). When examining the cortical activity in this animal using principal components analysis (PCA), Hits and Correct Rejections showed some segregation in the space defined by the first 3 principal components. However, the False Alarms seemed to be less clustered in the space during both the early and late periods (**Fig. 6b** right). When averaging across all discriminating animals, differences in whisking behavior and population spiking activity were negligible in the early grating interaction, however there was increased whisking and increased barrel cortex activity after punishment for False Alarms (**Fig. 6c**). We used the temporal decoders to examine if False Alarms were less discernible from Hits based on the cortical activity alone in the early period, which would be indicative that the cortical activity is relevant for orientation perception. Temporal decoders performed much worse in the early period at decoding the orientation category in Hit vs. False Alarm trials than they did for Hit vs. Correct Rejection trials (**Fig. 6d**). One explanation for this is that licking alone could drive the cortical neurons via induced whisker movements against the gratings, and the classifiers use this information to decode. If this was the case, the classifiers should also discriminate between False Alarms and Correct Rejections of a fixed stimulus, because in this situation only the licking behavior is different and not the stimulus. However, temporal decoders also performed much worse at discriminating False Alarms vs. Correction Rejections for matched stimuli than they did for discriminating Hits vs. Correct Rejections (**Fig. 6e**). There was an elevated baseline for discriminating False Alarms vs. Correct Rejections that could be related to task engagement, but after controlling for this baseline there was significantly less decoding in the early period than there was for Hits vs. Correction Rejections. In summary, on trials where the mice discriminate the gratings (HvCR), decoders also

performed best at discriminating the gratings (better than HvFA or FAvCR). These analyses thus establish a trial-by-trial link between discrimination in the barrel cortex population activity and correct decisions.

Discussion

We have shown that, like freely moving rats[19], head-fixed mice can be trained to discriminate tactile gratings based on orientation using only their whiskers (**Fig. 1**), and this perceptual process is barrel cortex-dependent (**Fig. 2**). The recognition of isotropic tactile features like orientation have received considerably less attention in whisker studies than texture-based features such as the coarseness of sandpapers[12–16,23]. However, there is evidence from behavioral studies in rodents that form-related tactile cues can also be used by animals to guide behavior[19,24]. Therefore, the establishment of perceptual tasks such as the discrimination of grating orientation, three-dimensional bar orientation[25], or surface concavity[26] will open up new lines of inquiry into the neural underpinnings of tactile object recognition. These new behavioral paradigms will be important to understand how different tactile inputs that are spread across space and time can be integrated to form a holistic tactile experience. As a proof of principle, from the coarseness studies in rodents and primates, a general motion-based mechanistic theory was postulated[1] that relied on temporal integration of sensor micromotions. These similarities likely extend to other tactile qualities, so the development of new tasks across different species is of broad interest.

To perform grating orientation discrimination in head-fixed conditions, mice need to execute a sequence of appropriate behaviors, much like humans do in object manipulation tasks[27]. The first action is to detect the incoming grating. In this pursuit,

we found that discriminating mice whisked vigorously when the grating was approaching (**Fig. 3**), which generated dynamic responses in barrel cortex neurons (**Figs. 3, 5a**). This anticipatory whisking behavior has also been reported during sandpaper discrimination in head-fixed mice[12,13]. Freely moving rodents also use goal-directed head movements along with exploratory whisking to perform tactile search[28], so the level of vigorous whisking observed here might be an adaptation to head-fixed task conditions. Once the approaching grating is localized, the mice must then refine their search behavior to adaptively sample the stimulus. During this period, the first traces of orientation tuning begin to appear in single neurons in the barrel cortex population (**Figs. 4-6**). Our results suggest that during detection and then search refinement, barrel cortex implements a flexible representation of grating orientation that starts as a temporal code, and as search is refined and decisive action is taken, stabilizes into a firing rate code. In the early grating interaction, temporal decoders outperformed rate decoders and mirrored concurrent psychophysical measurements (**Fig. 4**). Single neuron orientation tuning was rare and increased as licking set in (**Fig. 5**). This transformation from temporal to rate coding might depend on higher cortical areas or thalamocortical loops[29] that support information accumulation as the mouse interacts with the stimulus. Evidence accumulation models have recently been employed to study sandpaper discrimination in freely moving rats[18]. To apply these models to sandpaper discrimination, downstream processing beyond primary and secondary somatosensory cortex was postulated to integrate the information across volleys of incoming sensory information, each volley associated with a pump of the whiskers into the stimulus. Posterior parietal cortex (PPC) is an area downstream that might be the locus of this temporal integration. Electrophysiological recordings in PPC during

grating orientation discrimination in rats revealed that choice-related activity is present in single neurons[19], as well as graded orientation tuning similar to what we found in barrel cortex neurons (**Fig. 5, Supplementary Fig. 5**). The fine connectivity between PPC and the primary and secondary whisker areas is not well-documented but could provide blueprints on which to establish mechanistic models for tactile evidence accumulation, refinement, and decision.

The final action that the mouse needs to take after detection and search refinement is discriminative choice. When we examined orientation encoding by trial outcome instead of only by stimulus orientation, we found that false alarms were less distinguishable from Hits than Correct Rejections just before discriminative licking, and this could not be explained by differences in licking behavior alone (**Fig. 6**). Taken together, these observations indicate that the discriminability of the early temporal code in the barrel cortex mirrors the choice behavior of the animal on a trial-by-trial basis. Another report looking at the mouse's ability to detect single whisker deflections also found that barrel cortex neurons responded differently for different trial outcomes[30]. However, detection of a single whisker sinusoidal stimulus can be coded simply as the presence or absence of activity, and other studies have found that this kind of detection can be performed and even learned in the absence of barrel cortex[10,11]. Grating orientation is a tactile feature on a much different scale than the sinusoidal vibration of a single whisker, and the temporal population code that we uncover likely reflects the combination of grating contacts across whiskers and time, which is the raw information that needs to be integrated in order to recompose the orientation of the grating. The necessity of barrel cortex to discriminate gratings based on their orientation indicates that this integration relies on barrel cortex, and barrel cortex is dispensable for object detection. The fact that perceptual decisions

435 are predicted on a trial-by-trial basis by barrel cortex activity is in line with its causal
436 involvement and indicates that significant transformation of the raw stimulus
437 information is occurring from whiskers to cortex in this case, which is not the case in
438 detection tasks.

439 In summary, our results establish a cortex-dependent tactile discrimination
440 task in which the fine temporal dynamics of neural activity are informative, and
441 precisely define the timeline on which the temporal information is integrated to form a
442 percept. There is much to learn about the circuits that are responsible for this multi-
443 contact temporal integration and how they contribute to tactile object recognition.

444

445 ## Acknowledgements

446 This work was supported by the Paris-Saclay University (Lidex NeuroSaclay) and by
447 the International Human Frontier Science Program Organization (CDA-0064-2015, to
448 BB). AR is supported by the Fondation pour la Recherche Médicale
449 ECO20170637482. Valérie Ego-Stengel and Isabelle Férézou gave insightful advice
450 and feedback. The authors thank Guillaume Hucher for performing the histology and
451 Aurélie Daret for providing the animal care for the mice.

452 ## Author contributions

453 EH built the experimental setup, developed the behavioral task, carried out
454 behavioral experiments and electrophysiological recordings, did analysis, prepared
455 the figures and wrote the manuscript. AR did behavioral experiments, analysis, and
456 edited the manuscript. BB led the project, oversaw the analysis, and wrote the
457 manuscript.

458 ## Declaration of Interests

459 The authors declare no competing interests.

460

Figures

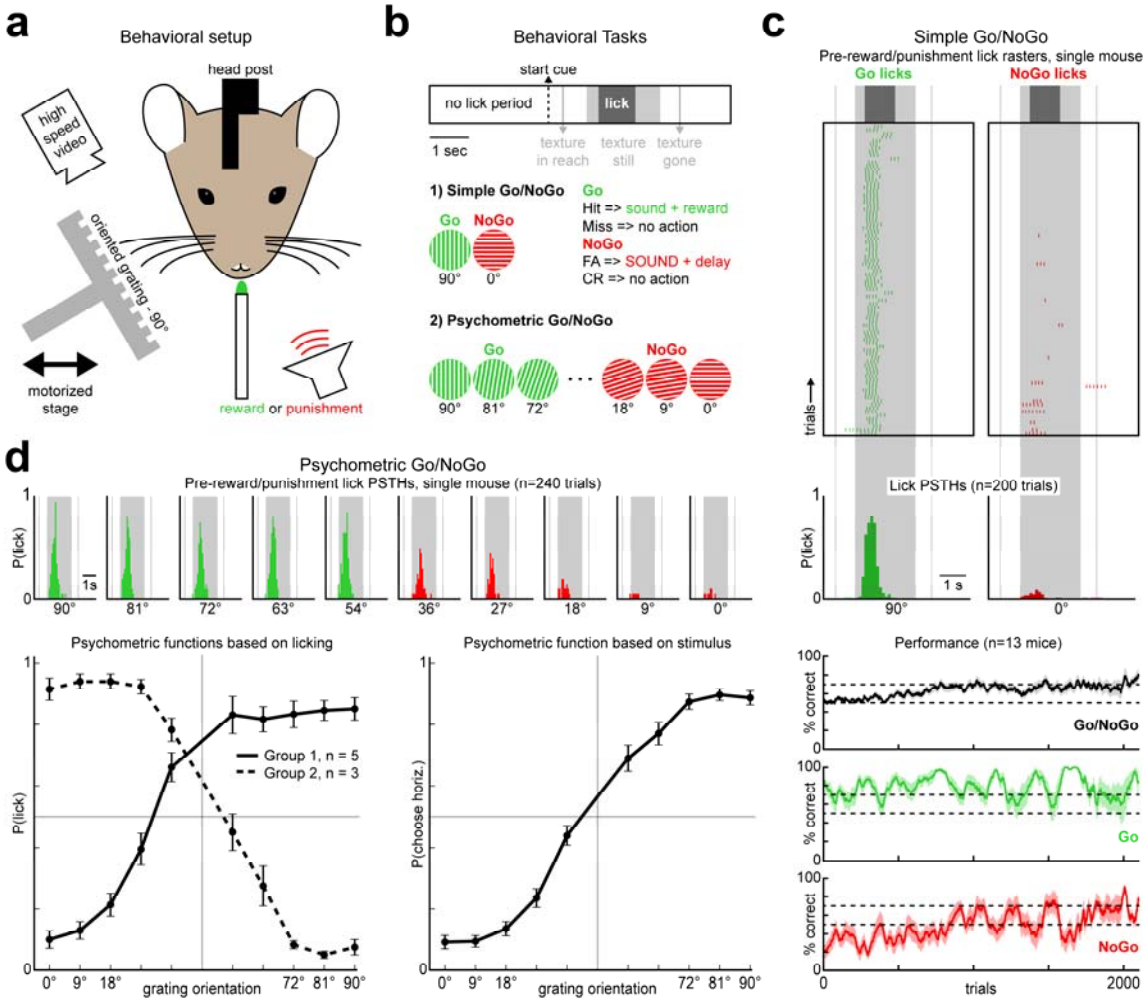

Figure 1 | Mice categorize texture gratings based on their orientation. a. A schematic showing the behavioral setup. **b.** Task parameters for (1) simple Go/NoGo discrimination and (2) psychometric Go/NoGo grating orientation discrimination tasks. **c.** Top: Lick raster from simple Go/NoGo discrimination between vertical (90°) and horizontal (0°) gratings. Middle: Lick probabilities from one session of simple Go/NoGo discrimination. Bottom: Mean learning curves (shaded areas are s.e.m., n=13 animals) for All (black), Go (green), and NoGo trials (red). **d.** Top: Lick probabilities from one session of psychometric Go/NoGo discrimination. Bottom left: Psychometric functions for two groups of mice where the Go/NoGo rules were

472 interchanged. Bottom right: The psychometric functions controlled for motivation
473 (error bars are s.e.m.).

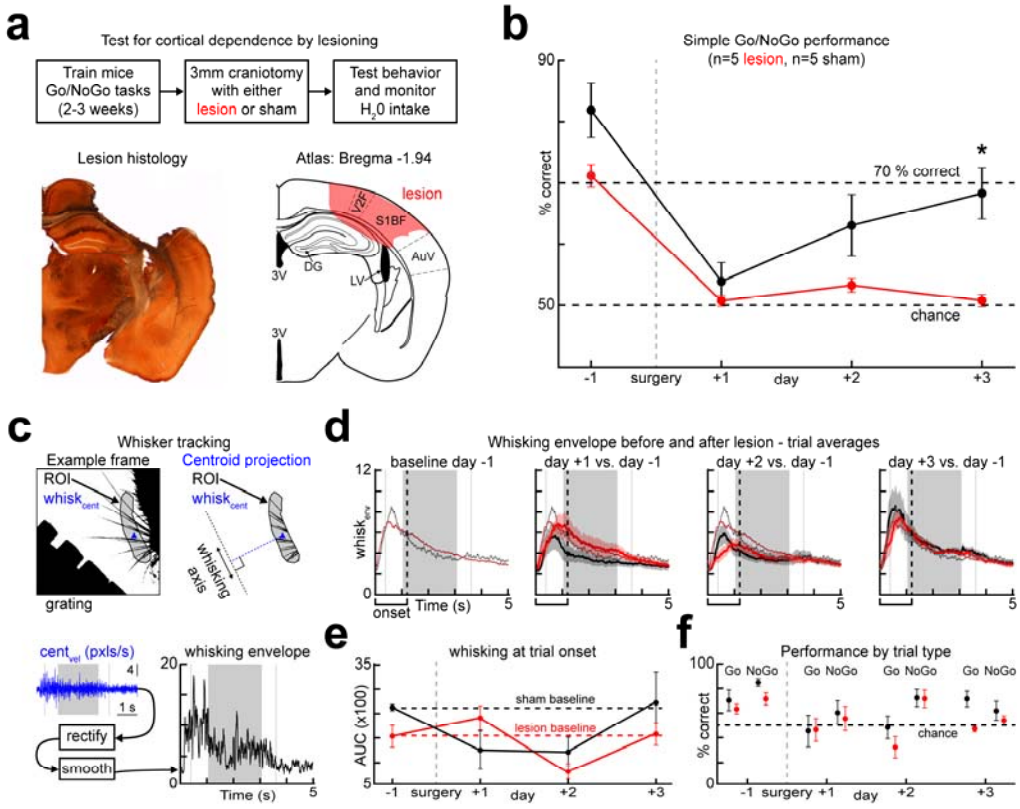

474

475 **Figure 2 | Barrel cortex is required for discriminating oriented gratings. a.** Top:
476 Experimental approach and timeline. Bottom left: An example barrel cortex lesion.
477 Bottom right: the corresponding slice in the brain atlas. Abbreviations: third ventricle
478 (3V), dentate gyrus (DG), lateral ventricle (LV). **b.** Simple Go/NoGo discrimination
479 performance before and after surgery in lesion and sham groups (p=0.0056,
480 bootstrap resample test). **c.** Whisker tracking during performance of the task. Top
481 left: A binarized frame. Top right: A manually selected region of interest (ROI)
482 containing the bases of the whiskers and the centroid (blue). Bottom left: the velocity
483 of the centroid plotted across a trial. Bottom right: the resulting whisking envelope
484 after rectification and smoothing. **d.** Top: Average whisking envelopes across days
485 for lesion and sham groups. **e.** Area under the curve (AUC) during the whisker search

period across days for lesion and sham groups. **f.** Performance broken down by trial type for lesion and sham groups.

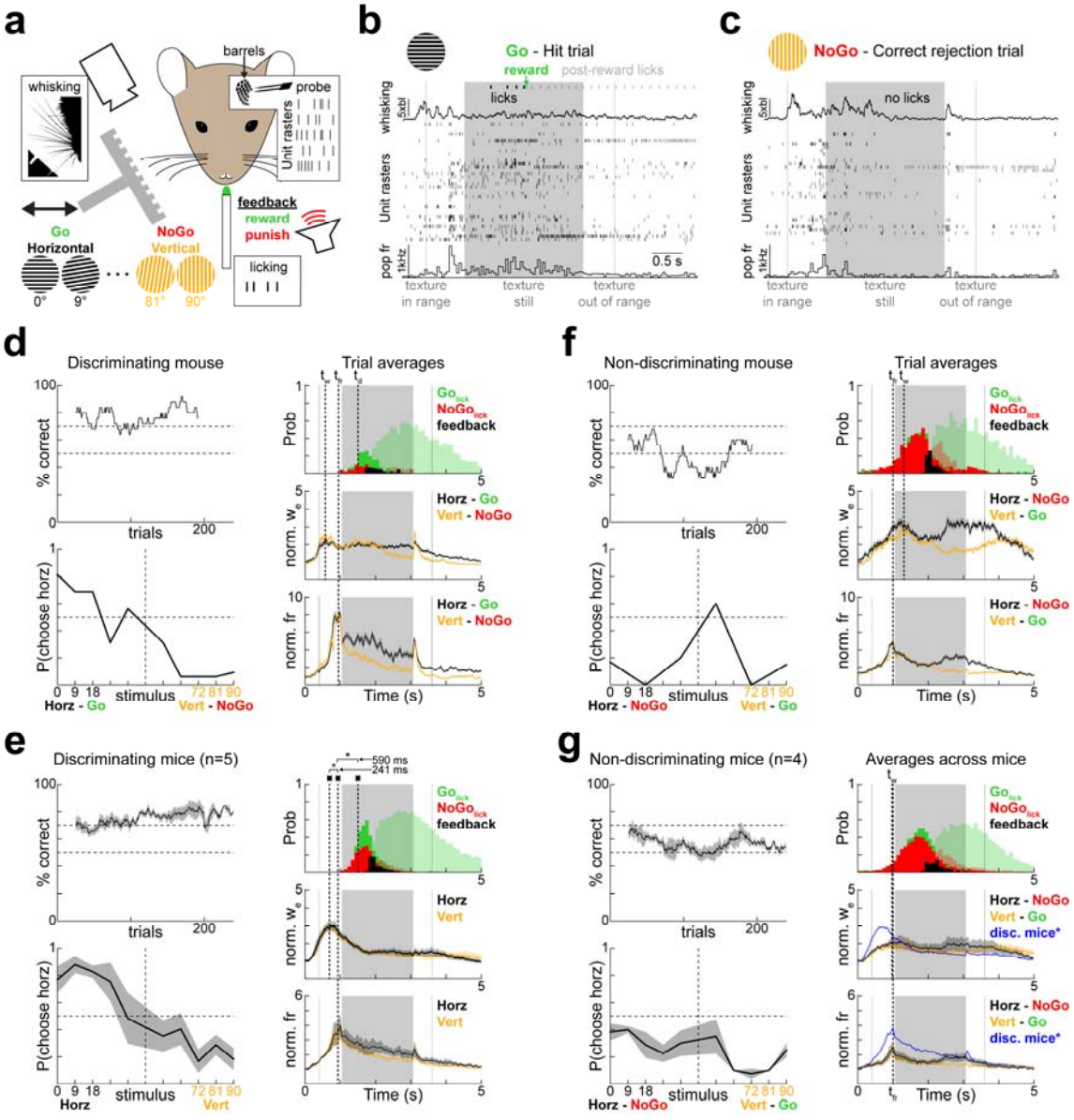

Figure 3 | Discrimination performance correlates with exploratory whisking and increased barrel cortex spiking activity. a. A schematic of the recording setup. **b.** An example hit trial showing licks, reward, whisking, and unit rasters. **d.** Same as B for a correct rejection trial. **d-e.** Performance across trials, psychometric functions, licking, whisking, and total population spiking activity for a discriminating mouse (d) or

494 5 discriminating mice (e). Shaded lick histograms are licks after reward/punishment.

495 Shading around curves is s.e.m. **f-g.** Same as d-e but for non-discriminating mice.

496

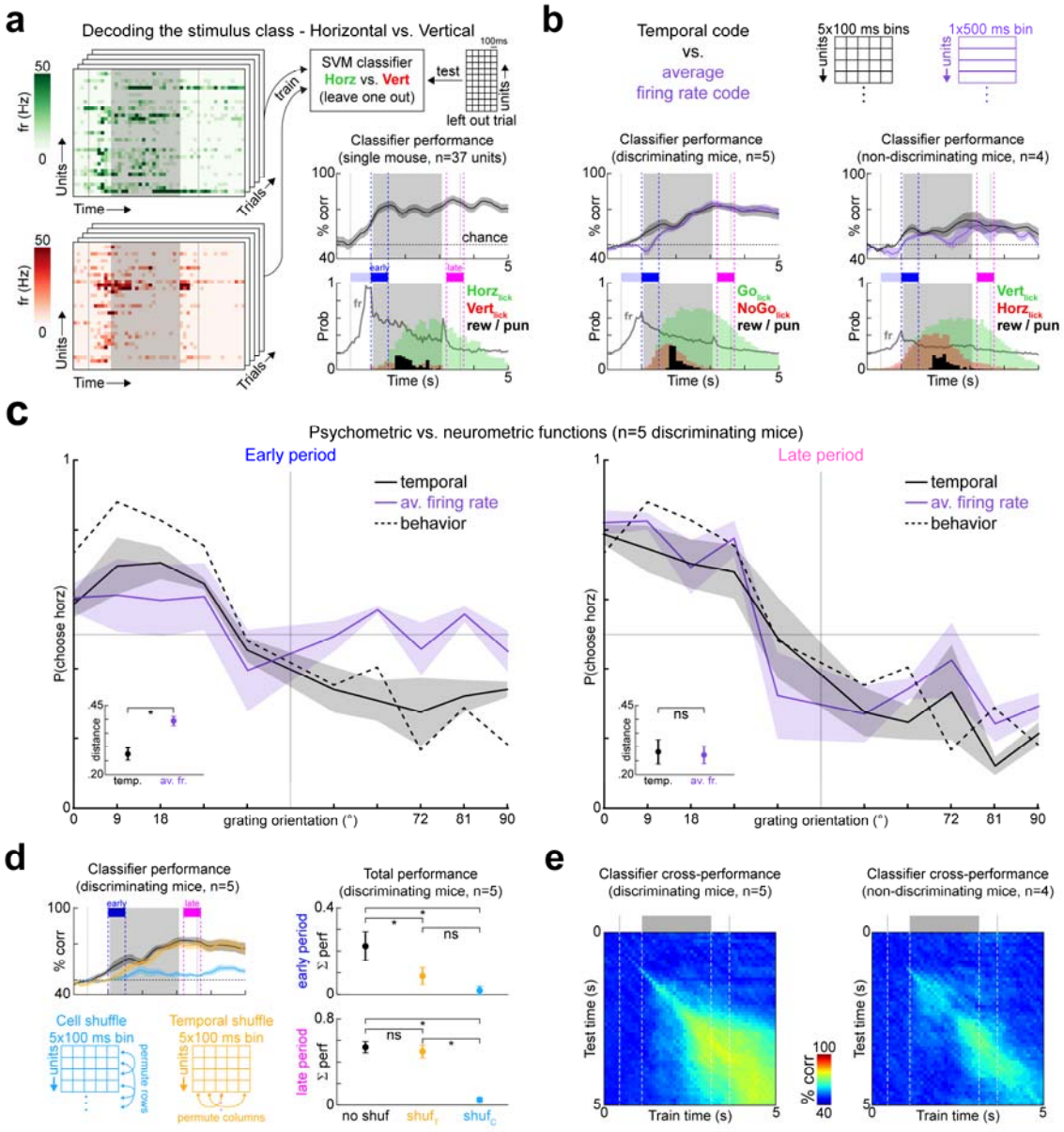

Figure 4 | Temporal decoders reproduce psychophysical measurements and outperform rate decoders during object search. a. Schematic showing how the support vector machine (SVM) classifiers were trained and tested for one example mouse. Classifier performance is aligned with the licking behavior and the population firing rates below. The early period is defined as the 500 ms before discriminative licking (across all trials) and the late period is the same size window but after reward or punishment has been given. **b.** Two classifier types defined by their bin

arrangements were tested on both the discriminating and the non-discriminating groups of mice: temporal (black) and average firing rate (purple). Performance, licking behavior and population firing rates are shown for the discriminating (left, n=5) and non-discriminating (right, n=4) groups of mice. **c.** Psychometric and neurometric functions for each classifier type based on the population activity in the early period (left) or the late period (right). Insets: Distances of the classifier neurometric curves from the behavior psychometric curves (early: p=0.0268, late: p=0.630, paired bootstrap resample test, see Methods). **d.** Total performance of the temporal decoders when either time (orange) or cell identity (light blue) is shuffled (early period: p=0.033 no shuffle vs. time, p=0.004 no shuffle vs. identity, and p=0.1876 for time vs. identity, late period: p=0.414 no shuffle vs. time, p=0.0014 no shuffle vs. identity, and p=0.0056 for time vs. identity, paired bootstrap resample test, see Methods). **e.** Classifier cross-performance when training and testing times are varied for discriminating and non-discriminating groups of mice.

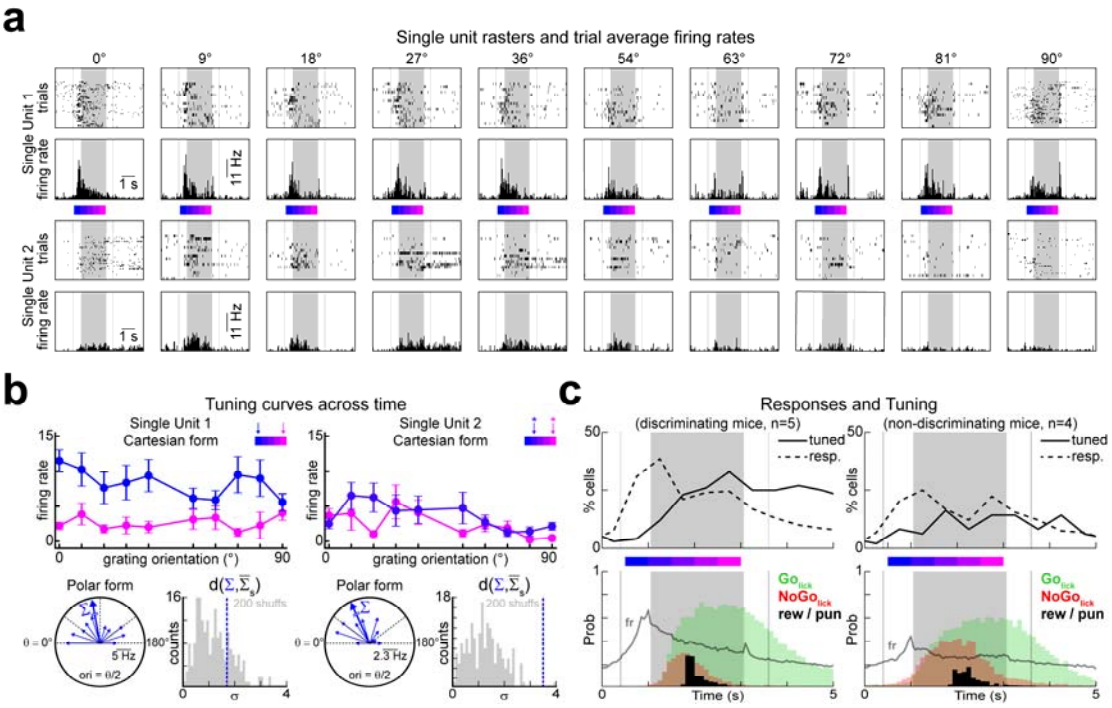

Figure 5 | Grating orientation tuning is weak at the onset of barrel cortex spiking responses but increases as licking sets in. a. Single trial rasters and trial-averaged PSTHs from two example single units during performance of the psychometric Go-NoGo task. **b.** Tuning curves from 2 example single units (same units from a) in various time windows color-coded by where the 500 ms time bin in which the curves were computed falls with respect to early vs. late periods. **c.** The percentage of responsive cells and orientation-tuned cells relative to trial onset. Population firing rates and licking behavior are plotted below to serve as a reference.

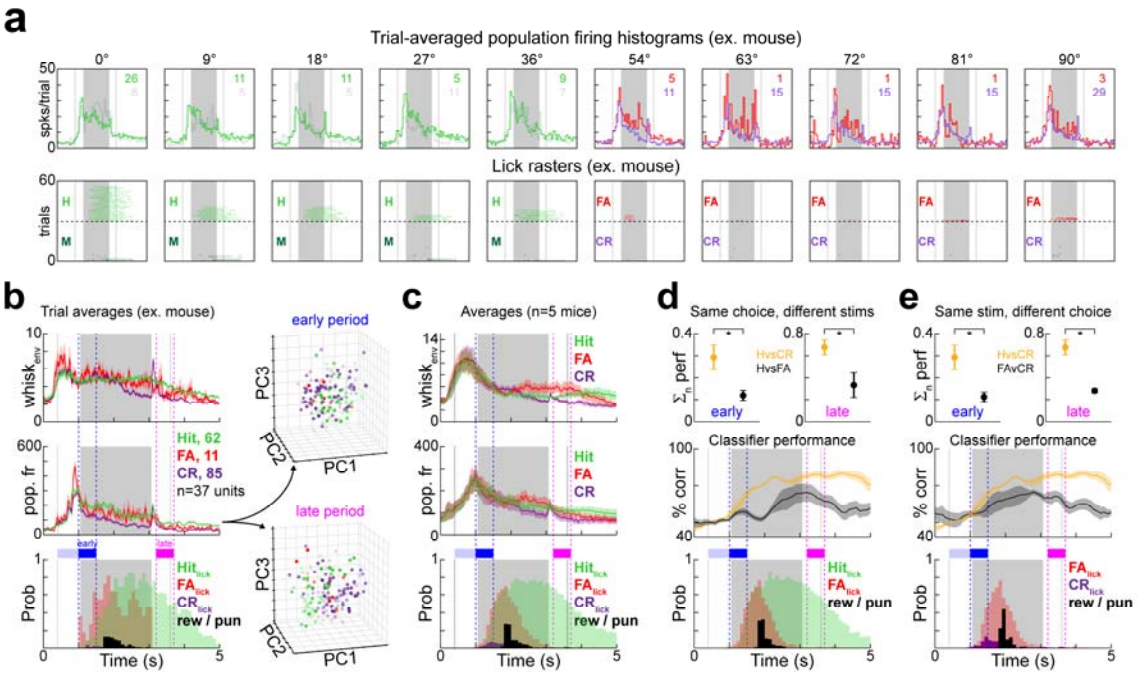

Figure 6 | Barrel cortex activity encodes trial outcome for correct decisions on a trial-by-trial basis controlling for licking. a. Top: Trial-averaged population firing rates separated by orientation and outcome (Hits, Misses, False Alarms, and Correct Rejections are lime green, dark green, red, and purple respectively) Bottom: Lick rasters for all trials. **b.** Left: Trial-averaged whisking envelope, population firing rate, and licking behavior separated for Hits (lime green), Correct Rejections (purple), and False Alarms (red) for an example mouse. Right: Population vectors projected onto the first three principal components for the early period (top) and the late period (bottom). **c.** Same as b for all discriminating mice (n=5). **d.** SVM classifier decoding for Hits vs. False Alarms (black) and Hits vs. Correct Rejections (gold). Top: total performance in the early and late periods for the different classifiers normalized to the baseline before trial start (p=0.0214 and p=0.035, paired bootstrap resample test), Middle: Classifier performance across all time points relative to trial onset. Bottom: Licking behavior for Hits and False Alarms. **e.** Same as d for False Alarms vs. Correct Rejections (p=0.018 and p=0.0134, paired bootstrap resample test).

References

1. Diamond, M. E. Texture sensation through the fingertips and the whiskers. *Current Opinion in Neurobiology* (2010). doi:10.1016/j.conb.2010.03.004
2. Maklad, A., Fritzsch, B. & Hansen, L. A. Innervation of the maxillary vibrissae in mice as revealed by anterograde and retrograde tract tracing. *Cell Tissue Res.* (2004). doi:10.1007/s00441-003-0816-z
3. Bosman, L. W. J. *et al.* Anatomical Pathways Involved in Generating and Sensing Rhythmic Whisker Movements. *Front. Integr. Neurosci.* **5**, 1–28 (2011).
4. Woolsey, T. A., Dierker, M. L. & Wann, D. F. Mouse SmI cortex: qualitative and quantitative classification of Golgi impregnated barrel neurons. *Proc. Natl. Acad. Sci. U. S. A.* (1975). doi:10.1073/pnas.72.6.2165
5. Petersen, C. C. H. The functional organization of the barrel cortex. *Neuron* (2007). doi:10.1016/j.neuron.2007.09.017
6. Kleinfeld, D., Ahissar, E. & Diamond, M. E. Active sensation: insights from the rodent vibrissa sensorimotor system. *Current Opinion in Neurobiology* (2006). doi:10.1016/j.conb.2006.06.009
7. Estebanez, L., Férézou, I., Ego-Stengel, V. & Shulz, D. E. Representation of tactile scenes in the rodent barrel cortex. *Neuroscience* (2018). doi:10.1016/j.neuroscience.2017.08.039
8. O'Connor, D. H. *et al.* Vibrissa-based object localization in head-fixed mice. *J. Neurosci.* (2010). doi:10.1523/JNEUROSCI.3762-09.2010
9. O'Connor, D. H., Peron, S. P., Huber, D. & Svoboda, K. Neural activity in barrel cortex underlying vibrissa-based object localization in mice. *Neuron* (2010). doi:10.1016/j.neuron.2010.08.026

10. Hutson, K. A. & Masterton, R. B. The sensory contribution of a single vibrissa's cortical barrel. *J. Neurophysiol.* (1986). doi:10.1152/jn.1986.56.4.1196

11. Hong, Y. K., Lacefield, C. O., Rodgers, C. C. & Bruno, R. M. Sensation, movement and learning in the absence of barrel cortex. *Nature* (2018). doi:10.1038/s41586-018-0527-y

12. Chen, J. L., Carta, S., Soldado-Magraner, J., Schneider, B. L. & Helmchen, F. Behaviour-dependent recruitment of long-range projection neurons in somatosensory cortex. *Nature* (2013). doi:10.1038/nature12236

13. Chen, J. L. *et al.* Pathway-specific reorganization of projection neurons in somatosensory cortex during learning. *Nat. Neurosci.* (2015). doi:10.1038/nn.4046

14. Chen, J. L., Voigt, F. F., Javadzadeh, M., Krueppel, R. & Helmchen, F. Long-range population dynamics of anatomically defined neocortical networks. *Elife* (2016). doi:10.7554/eLife.14679

15. Isett, B. R., Feasel, S. H., Lane, M. A. & Feldman, D. E. Slip-Based Coding of Local Shape and Texture in Mouse S1. *Neuron* (2018). doi:10.1016/j.neuron.2017.12.021

16. Jadhav, S. P., Wolfe, J. & Feldman, D. E. Sparse temporal coding of elementary tactile features during active whisker sensation. *Nat. Neurosci.* (2009). doi:10.1038/nn.2328

17. Zuo, Y., Perkon, I. & Diamond, M. E. Whisking and whisker kinematics during a texture classification task. *Philos. Trans. R. Soc. B Biol. Sci.* (2011). doi:10.1098/rstb.2011.0161

18. Zuo, Y. & Diamond, M. E. Texture Identification by Bounded Integration of Sensory Cortical Signals. *Curr. Biol.* (2019). doi:10.1016/j.cub.2019.03.017

19. Nikbakht, N., Tafreshiha, A., Zoccolan, D. & Diamond, M. E. Supralinear and Supramodal Integration of Visual and Tactile Signals in Rats: Psychophysics and Neuronal Mechanisms. *Neuron* (2018). doi:10.1016/j.neuron.2018.01.003

20. Bathellier, B., Ushakova, L. & Rumpel, S. Discrete Neocortical Dynamics Predict Behavioral Categorization of Sounds. *Neuron* (2012). doi:10.1016/j.neuron.2012.07.008

21. Ceballo, S., Piwkowska, Z., Bourg, J., Daret, A. & Bathellier, B. Targeted Cortical Manipulation of Auditory Perception. *Neuron* (2019). doi:10.1016/j.neuron.2019.09.043

22. Harvey, M. A., Sachdev, R. N. S. & Zeigler, H. P. Cortical barrel field ablation and unconditioned whisking kinematics. *Somatosens. Mot. Res.* (2001). doi:10.1080/01421590120072213

23. Garion, L. *et al.* Texture coarseness responsive neurons and their mapping in layer 2-3 of the rat barrel cortex in vivo. *Elife* (2014). doi:10.7554/eLife.03405

24. Anjum, F., Turni, H., Mulder, P. G. H., Van Der Burg, J. & Brecht, M. Tactile guidance of prey capture in Etruscan shrews. *Proc. Natl. Acad. Sci. U. S. A.* (2006). doi:10.1073/pnas.0605573103

25. Brown, J. *et al.* Spatial integration during active tactile sensation drives elementary shape perception. *bioRxiv* (2020). doi:10.1101/2020.03.16.994145

26. Nogueira, R., Rodgers, C. C., Fusi, S. & Bruno, R. M. Sensorimotor strategies and neuronal representations of whisker-based object recognition in mouse barrel cortex. in (2019). doi:10.32470/ccn.2019.1277-0

27. Johansson, R. S. & Flanagan, J. R. Coding and use of tactile signals from the fingertips in object manipulation tasks. *Nature Reviews Neuroscience* (2009). doi:10.1038/nrn2621

28. Schroeder, J. B. & Ritt, J. T. Selection of head and whisker coordination strategies during goal-oriented active touch. *J. Neurophysiol.* (2016). doi:10.1152/jn.00465.2015

29. Ahissar, E. Temporal-Code to Rate-Code Conversion by Neuronal Phase-Locked Loops. *Neural Comput.* (1998). doi:10.1162/089976698300017683

30. Kwon, S. E., Yang, H., Minamisawa, G. & O'Connor, D. H. Sensory and decision-related activity propagate in a cortical feedback loop during touch perception. *Nat. Neurosci.* (2016). doi:10.1038/nn.4356

Online Methods

Animal Care

All experiments were performed in accordance with the French Ethical Committee (Direction Générale de la Recherche et de l'Innovation) and European legislation (2010/63/EU). Procedures were approved by the French Ministry of Education in Research after consultation with the ethical committee #59 (authorization number 9714-2018011108392486). Mice were housed in cages in groups of 2-4 individuals with food available ad libitum on a 12/12 light-dark cycle with temperature kept at 23° C.

Behavioral Setup

Mice were trained in a custom-built behavioral setup that was interfaced using a National Instruments (NI) card (USB-6343) to control a linear stage (Newmark eTrack series) that brought the gratings within reach of the whiskers and an Arduino Uno to control stepper motors (Makeblock) for adjusting the orientation angle of the grating and a solenoid valve (LVM10R1-6B-1-Q, SMC) for delivering water rewards (5-8 µL). Sound cues were played with loudspeakers (Labtec Spin 85 speakers). Licking signals were acquired and digitized using a capacitive sensor (Sentronic AG, SK-3-

18/2,5-B-VA/PTFE) before being fed into the NI card. Software to carry out the training protocols and log the licking data was coded in Matlab using the data acquisition toolbox. Code is available upon request.

Headpost Implantation

To stabilize the animals in the behavioral apparatus, a head-fixation post was implanted along the mid-line of the skull. Mice (C57BL/6) that were 6-8 weeks old (20-26g) were anesthetized by intraperitoneal injection of a mix of ketamine (Ketasol, 80 mg/kg) and medetomidine (Domitor, 1 mg/kg). Once the mice were insensitive to hindpaw pinch, they were placed on a nose clamp and their eyes were kept moist with Ocrygel (TVM Lab). Body temperature was maintained at 36° using a thermal blanket. Xylocaine was injected under the skin in the center of the skull near bregma. Fur in the surgical location was removed using Veet, and a long incision was made in the skin along the midline of the skull 10 minutes after Xylocaine injection. After being fully exposed, the dorsal surface of the skull was scratched with a scalpel to create striations. The scratched skull was then cleaned with hydrogen peroxide. A head-fixation post was glued in place along the midline using cyanoacrylate, and then the exposed skull and base of the post were covered with Super-Bond (C&B, Sun Medical Co., Ltd.). The implant and all exposed surfaces were then embedded in dental cement. After everything had solidified, the mice were injected in one of the hindlimbs with 15 µL of atipamezole (Antisedan, Orion pharma) and transferred to a recovery cage that was placed on a heating blanket. Mice recovered for at least 1 week before any further manipulation.

Orientation discrimination training protocol

Mice were weighed every day during water deprivation periods to make sure they did not fall below 80% of pre-deprivation body mass. For two days before training, mice

were fully water deprived. On the first day of training, the mice were placed on the head-fixation post for 10 minutes in the dark with the lick port in reach. They were then given single water rewards (5-8 μL) randomly until they started to lick regularly at the lick port. Once they were comfortable licking the lick port for water reward, a protocol was launched that made one reward possible every 10 seconds if the animal licked to initiate the delivery, for up to a maximum of 100 rewards. After this habituation (1-2 days, 1 hour per day), the animals were given trials only with the Go grating until they licked regularly at the correct time within single trials. The trial timeline is shown in **Fig. 1**. For the first 40 trials, rewards were given automatically 1 second after the grating came into reach of the whiskers. After these free rewards, the mice had to lick in a 2 second window that started 1 second after the grating came into reach to receive the reward. The starting threshold to trigger reward was a single lick, which was then increased to as high as 4 (2-4 across all mice) licks to trigger a reward. If animals performed 3 misses in a row, the next Go trial automatically was rewarded, and this 'miss' counter was reset while the trial was still scored as a miss. Once the rewards were action-contingent within the trial framework, performance was tracked. When the animals were able to perform 70% correct across an entire training session, a NoGo stimulus was introduced the next day interleaved pseudo-randomly with the Go grating at a ratio of 3 Go trials for every 1 NoGo trial. If the addition of NoGo trials and their associated punishments (white noise at 60-70 dB and time out of 5-20 seconds) did not cease reward seeking behavior, the ratios were equilibrated (50% Go 50% NoGo) on the next day of training. The first NoGo stimulus was a flat surface (a small circle of printer paper glued on a disk the same dimensions as the gratings) with no grating (**Supplementary Fig. 1**). Once the animals discriminated this flat surface from the

Go grating (**Supplementary Fig. 1,** performed 70% correct across 200 trials in a single day), the NoGo stimulus was changed to a grating orthogonal to the Go grating. Punishments (loudness of the white noise and length of the time out) and lick thresholds were increased if animals could not refrain from licking for NoGo gratings. After 2 days of 70% performance in discriminating orthogonal gratings, intermediate grating orientations were introduced. At first, only 4 intermediate orientations (9, 18, 72, and 81°) were given, but then another 4 (27, 36, 54, and 63°) were added after performance stabilized above 70% correct. For the full psychometry, a single training session contained 40 trials for each extremity (0 and 90°) and 20 trials for each intermediate grating, for a total of 240 trials.

Task performance and psychophysics analysis

Learning curves across trials were calculated by dividing the number of correct responses (hits + correct rejections) in the preceding 25 trials by 25. Across days the curves were stitched together and smoothed with a Gaussian kernel. If the animals ceased licking for more than 15 trials, the trials were removed from the learning curves, as blocks of inactivity of this size indicate the mouse is distracted or satiated. Discriminative licking was detected by Wilcoxon rank-sum tests on the licking histograms (100 ms bins) generated for each trial (significance for $p<0.01$) comparing horizontal trials (<45°) with vertical trials (>45°) at each time bin. The first bin with a significant difference was taken as the 'discrimination time'. Psychometric functions in **Fig. 1d** were taken from 2 days of task performance (480 trials). The criteria for selecting these days was that total performance was above 70% correct across the entire day and there were not too many false alarm trials at the beginning of training (indicating over-thirst) or too many miss trials at the end of training (indicating satiation).

721 **Cortical lesions and histology**

722 After all mice learned to discriminate horizontal and vertical gratings (n=5 mice) and
723 some learned the full psychometric version of the task (n=2 out of the 5), they were
724 anesthetized (1.5% isoflurane delivered with Somnosuite, Kent Scientific) and placed
725 in a nose clamp. A thermal blanket kept body temperature above 36° C. Ocrygel
726 (TVM Lab) was applied the eyes to keep them from drying out. The location of the C2
727 barrel had been marked on the skull (A/P: -1.5mm, M/L: 0/3.3mm) from the headpost
728 implantation surgery in these mice, and this mark was used as the center of a 3-4
729 mm diameter craniotomy. Thermo-coagulation lesions were carried out with a fine
730 tipped cauterizer, making sure not to touch the surface of the brain, but to bring the
731 cauterizer just close enough to blacken the exposed cortical tissue containing the
732 barrel field. The craniotomy was then covered with Kwik-Cast (World precision
733 instruments), and then sealed with dental cement. Sham animals underwent the
734 same surgical procedure except they did not receive thermo-coagulation lesions.
735 After surgery and recuperation (~1 hour in a recovery cage), mice were given 250 µL
736 of water and returned to their home cages. The behavioral testing began again the
737 day after surgery. When behavioral testing was complete, lesioned mice were
738 transcardially perfused with saline followed by a 4% formaldehyde solution in 0.1 M
739 phosphate buffer (PB). Brains were dissected and then post-fixed overnight at 4° C.
740 After washing with phosphate-buffered saline (PBS), brains were cut into 80 µm
741 coronal slices. Slices were mounted and then imaged using a Nikon eclipse 90i
742 microscope (Intensilight, Nikon) and Nikon Pan UW objectives (1x/0.04 W.D 3.2 or
743 2x/0.06 W.D. 7.5). Slices were then manually aligned with the Paxinos mouse brain
744 atlas and the lesioned areas were tracked along the anterior-posterior axis to make
745 sure the covered the posterior-medial barrel field (**Supplementary Fig. 2**). Sham

mice were used later for electrophysiological recordings during task performance, after which their brains were treated in the same way, except they were sliced tangentially to reveal electrode locations with respect to the barrels (**Supplementary Fig. 3**). Electrode tracks in these preparations were visible because 1,1'-Dioctadecyl-3,3,3',3'-Tetramethylindocarbocyanine Perchlorate (DiI) was placed on the shanks before they were inserted into the brain.

Whisker movement tracking

During some sessions, high speed videos of the whisker interactions with the gratings were filmed with an infrared video camera (Baumer, 500 fps). The frames were grabbed on the same clock as the stimulus presentation to assure synchronization. For each session of whisker videos, a region of interest (ROI) was manually selected around the bases of the whiskers that were in focus. In this ROI, the centroid of the binarized whiskers was computed, and this centroid was then projected onto a line that was perpendicular to the rostral whiskers to give a single coordinate. The velocity of the centroid coordinate across frames was rectified and smoothed to give the whisking envelope. This quantifies the global rostral-caudal movement of all the whiskers. This procedure is graphically displayed in **Fig. 2c**. Normalization to whisking levels in the first 30 frames (first 60 ms of a trial) was sometimes applied to compare across mice with different levels of baseline whisking activity.

Electrophysiological recordings during task performance

On the day of the recording, mice were briefly anesthetized (30 minutes, 1% isoflurane delivered with Somnosuite, Kent Scientific) and the dental cement that was covering the craniotomies from the sham surgery (n=5 sham animals) was removed. In 4 other experiments, fresh craniotomies were drilled following the same protocols

771 described in the lesion section above (except no lesions). After durotomy, the
772 exposed cortical surface was moistened with fresh Ringer's solution and then
773 covered with Kwik-Cast (World precision instruments), which was secured in place
774 with cyanoacrylate. The mice were then allowed to recover for 2-3 hours in a cage
775 that was placed on a heating blanket. Mice were then placed in the behavioral setup
776 and the Kwik-Cast was carefully removed, making sure not to damage the brain in
777 the process. Multi-electrode silicon probes (A2x32 5mm-25-200-177, Neuronexus)
778 that had been coated with DiI were then slowly lowered into the left hemisphere
779 barrel cortex at about 2 μm per second. Once they reached a depth of 800-1000 μm
780 and sufficient spiking activity was seen across all channels. The preparation then
781 stabilized for 20 minutes before the behavioral protocol was launched, with periodic
782 water rewards given to keep the mice awake and unstressed. In 5 mice, intermediate
783 orientations were rewarded or punished and the number of trials for each orientation
784 followed the protocol detailed in the orientation discrimination training section. In 4
785 mice, intermediate orientations were given as catch trials, and in these experiments,
786 fewer intermediate orientation trials were given (90 horizontal trials, 90 vertical trials,
787 and 5 catch trials for each of 4 intermediate orientations). Psychometric data was
788 pooled across these 9 mice for the electrophysiological data set. For the behavior
789 alone (**Fig. 1**), all animals followed the same protocols that are described in the
790 orientation discrimination training section.

791 **Data processing and analysis for electrophysiological recordings**

792 Extracellular signals were acquired at 20kHz with an Intan RHD2000 recording
793 system. The raw data was median filtered to remove common mode noise from all
794 channels and then passed into KiloSort2 for spike detection and clustering. Clusters
795 were manually curated to pick out waveforms with physiological shapes that decay

with distance from a primary electrode (electrode with the largest magnitude waveform). The units that passed visual inspection and entered the analysis pipeline were both single units and multi-units depending on the refractory periods found in their autocorrelograms. Data from single and multi-units was pooled for all analyses. Trial-averaged spiking histograms were created by binning spikes in 50 ms bins (**Fig. 3**). Normalized firing rates were computed by dividing by the baseline firing rate, which was taken as the mean firing rate across 500 ms beginning 1 second before trial start.

Orientation tuning and response detection

Orientation tuning curves were constructed by breaking trials up into 500 ms blocks. For each unit and each 500 ms block, the total number of spikes for a stimulus of a given orientation determined the magnitude of the vector pulling in that direction in a polar coordinate system where all the orientation angles were multiplied by 2. The vector sum of these 10 (or 6) oriented vectors (0, 18, 36, 54, 72, 108, 126, 144, 162, 180° or 0, 36, 72, 108, 144, 180°) was compared to the distribution of vector sums obtained by shuffling the trial labels 200 times. If the actual vector sum was outside of the sphere defined by 95% of the 200 shuffles ($p<0.05$), then the cell was called orientation tuned in that 500 ms block. False positive rates were thus kept at 5%. Cells were deemed significantly responsive if evoked firing rates were 5 standard deviations above the baseline firing rate.

Defining the early period and late period

Significant differences in licking behavior were assessed by binning the digital lick signal counts into 100 ms bins. Then, the distributions of Go trial licks and NoGo trial licks were compared at each time point relative to trial onset using Wilcoxon rank sum tests, and the first time point in the trials that gave a significant result with

821 $p<0.01$ is where the mouse was said to have licked discriminatively. For each mouse,
822 the 500 ms before this time point were counted as the early period. The late period
823 was a fixed period after reward or punishment in which the animals had stopped
824 licking for the False Alarms but the texture was still in reach of the whiskers.

825 **Support vector machine (SVM) classifiers**

826 Spikes were placed into 100 ms bins to generate population vectors of various types
827 for each trial (**Fig. 4a**). The trials were divided either by grating orientation (**Fig. 4**) or
828 by trial outcome (**Fig. 6**). Binary non-linear SVMs were then trained using the sklearn
829 module in python along with the leave one out protocol in the model selection
830 subdirectory of this module. The non-linear classifiers used a gamma function with an
831 input parameter of 1/n_features (the 'auto' option from the sklearn documentation).
832 For each time step in the trials (100 ms), the classifiers were retrained based on the
833 corresponding subspaces of the population vectors just before that time step, and the
834 performance was the percentage of all trials correctly classified. Each trial was left
835 out only once. Principal components analysis (**Fig. 6**) on the population vectors was
836 done for an example mouse by taking all population vectors across all time for all
837 trials. The covariance matrix across the 185-dimensional space (37 neurons x 5 time
838 bins) was singular value decomposed and the top 3 singular vectors were then used
839 to visualize the data.

840 **Bootstrap resample test**

841 For small sample sizes (n=5) that are common in challenging experimental conditions
842 such as these, the most appropriate statistical test is non-parametric bootstrap
843 resampling. Wilcoxon and Mann-Whitney tests are often inappropriately used and
844 demand larger sample sizes (n>20). To carry out this test, we resampled 1000 times
845 with replacement from the pool of N (usually 5) mice and permuted the labels of what

was being tested (lesion vs. sham, temporal decoders vs. average firing rate decoders, etc). When appropriate, the permutations were done while keeping the measurements paired. If the difference of the mean values obtained was > or < 95% of the shuffled resampled mean differences, then the measurement was deemed significant with $p<0.05$. Exact p-values are provided as averages of 5 different resamples comprised of 1000 shuffles each.